

## Article

# Remazol Black Decontamination Study Using a Novel One-Pot Synthesized S and Co Co-Doped TiO<sub>2</sub> Photocatalyst

Riska Dwiyanca , Roto Roto  and Endang Tri Wahyuni \* 

Department of Chemistry, Faculty of Mathematics and Natural Sciences, Universitas Gadjah Mada-Sekip Utara, Bulaksumur, Yogyakarta 55281, Indonesia; riska.dwiyanca@mail.ugm.ac.id (R.D.); roto05@ugm.ac.id (R.R.)

\* Correspondence: endang\_triw@ugm.ac.id; Tel.: +62-81328892114

**Abstract:** This study investigated the decolorization of Remazol Black (RBB) using a TiO<sub>2</sub> photocatalyst modified by S and Co co-doped TiO<sub>2</sub> (S-Co-TiO<sub>2</sub>) from a single precursor. X-ray diffraction, Fourier transform infrared spectroscopy, scanning electron microscopy, and UV-Vis specular reflectance spectroscopy were used to characterize the photocatalysts. The results revealed that the band-gap energy of the doped and co-doped TiO<sub>2</sub> decreased, with the S-Co-TiO<sub>2</sub> 8% showing the greatest one, and was found to be 2.78 eV while undoped TiO<sub>2</sub> was 3.20 eV. The presence of S and Co was also identified through SEM-EDX. An activity study on RBB removal revealed that the S-Co-TiO<sub>2</sub> photocatalyst showed the best result compared to undoped TiO<sub>2</sub>, S-TiO<sub>2</sub>, and Co-TiO<sub>2</sub>. The S-Co-TiO<sub>2</sub> 8% photocatalyst reduced RBB concentration (20 mg L<sup>-1</sup>) up to 96% after 90 min of visible light irradiation, whereas S-TiO<sub>2</sub>, Co-TiO<sub>2</sub>, and undoped TiO<sub>2</sub> reduced it to 89%, 56%, and 39%, respectively. A pH optimization study showed that the optimum pH of RBB decolorization by S-Co-TiO<sub>2</sub> was 3.0, the optimum mass was 0.6 g L<sup>-1</sup>, and reuse studies show that S-Co-TiO<sub>2</sub> 8% has the potential to be used repeatedly to remove colored pollutants. The results obtained indicate that the modification of S, Co co-doped titania synthesized using a single precursor has been successfully carried out and showed excellent characteristics and activity compared to undoped or doped TiO<sub>2</sub>.



**Citation:** Dwiyanca, R.; Roto, R.; Wahyuni, E.T. Remazol Black Decontamination Study Using a Novel One-Pot Synthesized S and Co Co-Doped TiO<sub>2</sub> Photocatalyst. *Photochem* **2021**, *1*, 488–504. <https://doi.org/10.3390/photochem1030032>

Received: 4 November 2021

Accepted: 23 November 2021

Published: 26 November 2021

**Publisher's Note:** MDPI stays neutral with regard to jurisdictional claims in published maps and institutional affiliations.



**Copyright:** © 2021 by the authors. Licensee MDPI, Basel, Switzerland. This article is an open access article distributed under the terms and conditions of the Creative Commons Attribution (CC BY) license (<https://creativecommons.org/licenses/by/4.0/>).

**Keywords:** cobalt; decolorization; photocatalyst; Remazol Black; sulfur; TiO<sub>2</sub>

## 1. Introduction

Dyestuff waste is a significant source of contamination in the aquatic environment. Among various synthetic dyes, Remazol Black (RBB) is the most widely used because of its low energy consumption during the dyeing process, water fastness, color brightness, and good fixation characteristics on fabric fibers [1,2]. However, due to its complex chemical structure, this dye is stable and difficult to biodegrade, so the concentration in the environment does not tend to decrease [3–6]. The release of this dye into the environment is extremely hazardous because it can produce toxic, mutagenic, and harmful by-products of oxidation, hydrolysis, and other chemical reactions that occur in the wastewater mixture, which are toxic, mutagenic, and harmful to microorganisms, aquatic life, and humans [5]. Therefore, an efficient method is needed to remove the dye concentration from wastewater before being discharged into the environment.

One of the effective methods for dealing with various organic pollutants such as dyestuff waste is advanced oxidation processes (AOPs) using heterogeneous photocatalysts [7,8]. Compared to other semiconductors, TiO<sub>2</sub> is the most widely used due to its advantages such as high photocatalytic activity, stability, non-toxicity, and low cost, and it has been widely used for environmental pollution control, especially water pollution by dyestuff waste [9,10]. However, due to its large band gap (anatase 3.2 eV), TiO<sub>2</sub> can only be activated by UV radiation, which is only 3–4% of the available total solar radiation. To improve the efficiency of photocatalyst activity in the visible light region, TiO<sub>2</sub> should be further modified [11–13].

Modification with dopants has been shown to reduce the band-gap energy and increase the responsivity of TiO<sub>2</sub> to the visible light region. The use of single dopants has been widely studied. However, there are several drawbacks to the effects of single doping, including that high doping levels are almost unattainable due to the mismatch of ionic charge and/or atomic radius of the dopants with TiO<sub>2</sub>, thermal instability, and the rate of electron recombination being increased compared to undoped conditions [14], which can inhibit the photocatalytic activity of TiO<sub>2</sub>. Co-doping can be an alternative to solve this problem. The co-doping technique is an effective method for lowering the band gap energy of TiO<sub>2</sub>, allowing TiO<sub>2</sub> to be responsive in the visible light range [15–18]. Meanwhile, the combination of metallic and non-metallic dopants proved to be effective in reducing the band gap energy of TiO<sub>2</sub> significantly, reducing electron and hole recombination that might result from a single doping effect, thereby increasing photocatalytic activity in the visible spectrum for efficient utilization of sunlight [19].

Compared to other non-metallic dopants such as N and C, sulfur is considered advantageous due to its ability to narrow the band gap, high thermal stability, and enhanced photocatalytic activity [10,20–22]. Meanwhile, incorporation of 3D transition metals into TiO<sub>2</sub> is also an effective approach to reducing the band gap energy. The unfilled d-electron structure in transition metals can accommodate more electrons, allowing transition dopants to act as a photogenerated electron–hole pair trap, reducing the occurrence of electron–hole pair recombination on the photocatalyst surface [23]. Among other transition metals such as V, Cr, Mn, Fe, and Co, cobalt is considered a good candidate for TiO<sub>2</sub> doping due to the similarity of the ionic radius of Co<sup>2+</sup> to Ti<sup>4+</sup>, and it has been shown to increase the photocatalytic activity of TiO<sub>2</sub> in the visible region [24–26]. Co-doping modification of TiO<sub>2</sub> with S and Co has been reported. However, to the best of our knowledge, no studies have reported the use of a single precursor as a source of S and Co dopant, as well as activity assays for photocatalytic decontamination of Remazol Black under visible light exposure. Furthermore, we developed light-emitting diodes (LED) as a light source due to their long lifetime and high energy efficiency compared to typical light sources such as Xe lamps and Hg-Xe lamps [27].

## 2. Materials and Methods

### 2.1. Materials

Titanium(IV) isopropoxide (TTIP, 97%) was purchased from Hangzhou Jiu Peng Material Co., Ltd. (Zhejiang, China). Ethanol (C<sub>2</sub>H<sub>5</sub>OH, 99.5%), cobalt(II) sulfate (CoSO<sub>4</sub>), thiourea (CH<sub>4</sub>N<sub>2</sub>S), cobalt(II) chloride hexahydrate (CoCl<sub>2</sub>·6H<sub>2</sub>O), hydrochloric acid (HCl, 36%), sodium hydroxide (NaOH), and Remazol Black (RBB, C<sub>26</sub>H<sub>21</sub>O<sub>19</sub>N<sub>5</sub>S<sub>6</sub>Na<sub>4</sub>, MW = 991.82 g mol<sup>-1</sup>) were obtained from Merck, and deionized water was used in this work. The chemical structure of RBB is shown in Figure S1.

### 2.2. Synthesis of Photocatalysts

The sol-gel method was used to synthesize all of the photocatalysts. Under magnetic stirring, titanium(IV) isopropoxide (97%) was stoichiometrically dissolved in 20 mL ethanol. In separate bins, 0.24 g of thiourea was dissolved in a mixture of distilled water and ethanol (1:1 volume ratio) to obtain a dopant concentration of 10% S (*w/w*). The prepared TTIP solution was added dropwise to this solution under magnetic stirring, and the pH of the solution was adjusted to 3 with the addition of 1 M HCl. Stirring was continued for 2 h, and then the mixture was allowed to stand for 24 h for the gel ripening process. Then, the gel that formed was dried in an oven at 80 °C for 4 h, and the solid obtained was calcined at 450 °C for 3 h. The catalyst obtained was labeled S-TiO<sub>2</sub>.

To synthesize Co-doped TiO<sub>2</sub>, a similar method to the previous one was used. CoCl<sub>2</sub>·6H<sub>2</sub>O 4% (*w/w*) as a source of Co dopant was dissolved into a mixture of distilled water and ethanol to obtain a solution of Co. The prepared titanium solution was added dropwise into this dopant solution, followed by a similar procedure for the S-TiO<sub>2</sub> synthesis, and then the catalyst was marked as Co-TiO<sub>2</sub>.

To synthesize S and Co co-doped TiO<sub>2</sub>, a stoichiometric amount of titanium(IV) isopropoxide was dissolved in ethanol absolute under magnetic stirring (solution A). At the same time, 47.91 mg of CoSO<sub>4</sub> was dissolved in a mixture of distilled water and ethanol (volume ratio 1:1) to obtain the desired ratio of 4% (*w/w*) Ti: CoSO<sub>4</sub> dopant concentration (solution B). Solution A was added dropwise to solution B under magnetic stirring, then the solution pH was adjusted to 3.0 with the addition of 1 M HCl, and stirring continued for 6 h, followed by aging for 24 h. Afterward, the gels were dried at 80 °C for 4 h to evaporate water and organic materials. Then, dry gels were calcined at 450 °C for 3 h to control the crystal phase of the catalyst. The final catalyst was thoroughly milled and labeled as S-Co-TiO<sub>2</sub> 2%. A similar procedure was followed to prepare S-Co-TiO<sub>2</sub> with concentration ratios of 6%, 8%, and pure TiO<sub>2</sub> without adding dopants.

### 2.3. Photocatalyst Characterization

The composition and crystalline phase of the photocatalyst was identified by X-ray diffractometer (XRD Shimadzu 6000, Cu K $\alpha$  radiation  $\lambda = 0.15406$  nm as the source of X-rays, operated at 40 kV, 30 mA, the angular range of  $2\theta = 5\text{--}90^\circ$  and nickel as the filter). The crystallite size of the prepared photocatalyst was estimated by Scherrer equation (Equation (1)):

$$D = \frac{k\lambda}{\beta \cos\theta} \quad (1)$$

where  $k$  is a shape factor (0.94),  $\lambda$  is the wavelength of Cu K $\alpha$  source used,  $\beta$  is the full width at half maximum (FWHM), and  $\theta$  is the angle of diffraction.

A Fourier-Transform Infrared (FTIR) spectrophotometer (Shimadzu Prestige 21) was used to verify the functional groups and chemical bonds in the photocatalyst in the wavenumber 400–4000 cm<sup>-1</sup>. Scanning Electron Microscopy (SEM) equipped with Energy Dispersive X-ray Analysis (EDX) was used to determine nanoparticle morphology and nanoparticle composition, and to identify the photocatalyst light absorption profiles, UV-Vis Specular Reflectance Spectroscopy (UV-Vis SRS) was used.

### 2.4. Photocatalytic Activity

The photocatalytic activity of the synthesized S-Co-TiO<sub>2</sub> was studied for Remazol Black (RBB) decolorization using a batch system in a closed reactor equipped with 4 UV lamps (@20 W, intensity 200 lm/m<sup>2</sup>) and 4 visible lamps (TL-D, intensity @20 W, 2000 lm/m<sup>2</sup>), which can be adjusted for use (Figure S2). For comparison, photocatalytic activity tests were performed under the same conditions on other prepared photocatalysts TiO<sub>2</sub>, S-TiO<sub>2</sub>, and Co-TiO<sub>2</sub>. The variables studied included the type of photocatalyst, light source, initial pH, photocatalyst dose, dye concentration, and photocatalyst reuse test. In the study of light source parameters, visible light or UV light can be adjusted as needed, so the visible and UV tests were carried out under different conditions. At the beginning of the photocatalytic reaction, the prepared photocatalyst was dispersed in RBB solution and then magnetically stirred for 30 min in the dark without irradiation to achieve adsorption-desorption equilibrium conditions. The following process is a photocatalytic reaction initiated by contacting the solution with visible/UV light under continuous stirring. The photocatalyst was separated from the solution by centrifugation at 5000 rpm for 10 min at certain time intervals. Furthermore, the residual concentration after the photocatalytic process was investigated using a UV-Vis spectrophotometer at a wavelength of 598 nm ( $\lambda_{\max} = 598$  nm). The efficiency of RBB removal by photocatalyst was determined using Equation (3):

$$\text{The removal efficiency of RBB (\%)} = \frac{C_i - C_f}{C_i} 100 \quad (2)$$

where  $C_i$  was the initial RBB concentration (mg L<sup>-1</sup>) and  $C_f$  was the final RBB concentration (mg L<sup>-1</sup>). Each experiment was repeated four times.

### 2.5. pH Point of Zero Charge ( $pH_{PZC}$ ) of $TiO_2$ -S-Co

$pH_{PZC}$  of S-Co- $TiO_2$  was determined using the procedures from previous work [28] with a few modifications. A 0.1 g measure of catalyst was added to 25 mL 0.1 M  $NaNO_3$ . The pH of the solution was adjusted by adding HCl or NaOH solution to obtain pH values in the range of 2–11. The final pH values of the solution were determined after constant shaking for 2 h at 293 K and left for 24 h.

## 3. Results and Discussion

### 3.1. Photocatalyst Characterization

#### 3.1.1. XRD Analysis

The crystal phase of the photocatalyst was analyzed using XRD, and the XRD pattern is shown in Figure 1. The diffraction pattern of pure  $TiO_2$ , S- $TiO_2$ , Co- $TiO_2$ , and co-doped S-Co- $TiO_2$  showed the major peaks of the crystal planes for (101), (004), (200), (105), (211), (204), and (215) corresponded to the anatase phase of  $TiO_2$  (JCPDS reference No. 21-1272), and no other phases such as rutile or brookite appeared in the samples.

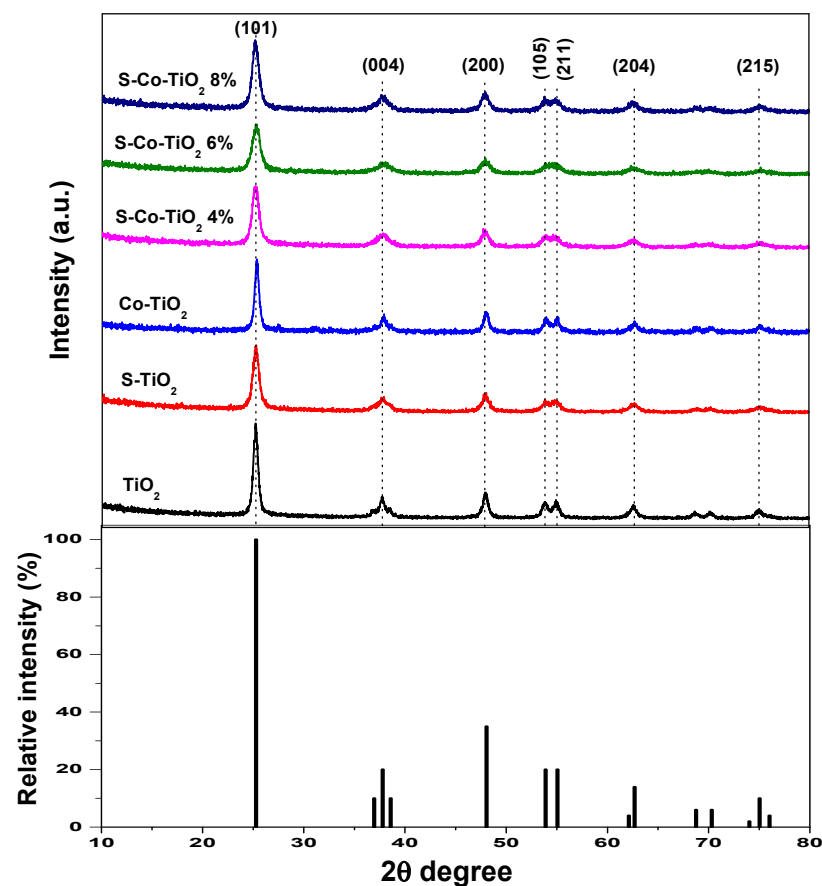


Figure 1. XRD pattern of undoped, doped, and co-doped  $TiO_2$  photocatalyst.

There were no other crystallite peaks for S and Co ions in any samples, indicating that the S and Co dopants were evenly distributed on the titania surface [15]. Furthermore, the diffraction peaks of doped and co-doped samples shifted narrowly to a larger diffraction angle, followed by a decrease in peak intensity compared to undoped  $TiO_2$ . The difference was also observed in the average crystallite size ( $D$ ) (Table 1), which is estimated using Scherrer's equation (Equation (1)). It was shown that the presence of dopant reduced the average crystallite size, with the most significant decrease attributed to the co-doping effect. As previously reported, the shift in diffraction peaks accompanied by a decrease in intensity and the average crystallite size after co-doping can be attributed to the presence

of new bonds formed after the addition of sulfur and cobalt dopant to titania, in the form of Ti–O–S or Ti–O–Co bonds or both, which suppresses titania crystal growth and causes distortion of the crystal structure [25,29,30].

**Table 1.** The average crystallite sizes and the band gap energy of undoped TiO<sub>2</sub> and S-TiO<sub>2</sub>, Co-TiO<sub>2</sub>, and S-Co-TiO<sub>2</sub>.

Photocatalyst	<i>D</i> (nm)	Band Gap (eV)
TiO <sub>2</sub>	5.154	3.20
S-TiO <sub>2</sub>	3.504	3.16
Co-TiO <sub>2</sub>	5.170	3.15
S-Co-TiO <sub>2</sub> 4%	2.405	2.82
S-Co-TiO <sub>2</sub> 6%	2.079	2.83
S-Co-TiO <sub>2</sub> 8%	2.445	2.78

### 3.1.2. FTIR Analysis

The functional groups formed on the photocatalyst before and after doped and co-doping were identified using the FTIR spectrum (Figure 2). Based on Figure 2, the spectrum of undoped TiO<sub>2</sub> displayed a broad absorption band at 3400–3600 and 1635 cm<sup>-1</sup>, which were identified as stretching and bending vibrations of the hydroxyl groups on the TiO<sub>2</sub> surface [20]. The adsorption band at 2924 cm<sup>-1</sup> was defined as the Ti–OH<sub>2</sub> group vibration, and the strong absorption band at 500–800 cm<sup>-1</sup> was defined for Ti–O strain vibrations [31]. In the S-TiO<sub>2</sub> and Co-TiO<sub>2</sub> doped samples, the Ti–O absorption band widens and shifts slightly to a lower wavenumber due to the substitution of Ti<sup>4+</sup> ions by Co<sup>2+</sup> ions [32] and Ti<sup>4+</sup> by S<sup>6+</sup>/S<sup>4+</sup> ions [33,34]. A more significant shift occurred in the S-Co-TiO<sub>2</sub> sample, which was associated with the substitution of the Ti<sup>4+</sup> ion by the two dopants S<sup>6+</sup> and Co<sup>2+</sup> ions. This replacement caused more defects, particularly oxygen vacancies, due to the charge neutrality after the replacement of Ti<sup>4+</sup> by Co<sup>2+</sup> or/and S<sup>6+</sup>/S<sup>4+</sup> [32,35]. Then, in the S-TiO<sub>2</sub> and S-Co-TiO<sub>2</sub> samples, a new peak appeared at 1047–1080 cm<sup>-1</sup>, which corresponds to the bending vibration of Ti–O–S. This bond is formed from the substitution of Ti<sup>4+</sup> by S<sup>6+</sup>/S<sup>4+</sup>, which also causes the Ti–O bond to weaken [36]. Furthermore, the peak at 1120–1125 cm<sup>-1</sup> confirmed the S–O bending vibration in the form of SO<sub>4</sub><sup>2-</sup>, indicating that S was presented in cationic species (S<sup>6+</sup>/S<sup>4+</sup>) since the substitution of Ti<sup>4+</sup> by S<sup>6+</sup>/S<sup>4+</sup> is chemically more favorable than the substitution of O<sup>2-</sup> by S<sup>2-</sup> (anionic sulfur), because of the ionic radius of S<sup>2-</sup> (1.7 Å) is quite larger than O<sup>2-</sup> (1.22 Å), so this substitution is difficult to achieve compared to the substitution by the cationic sulfur [20,34]. Meanwhile, the shift in the Ti–O absorption peak was greater in the co-doped sample than the doped sample, indicating that more Ti ions were replaced by S and Co dopants [15,18].

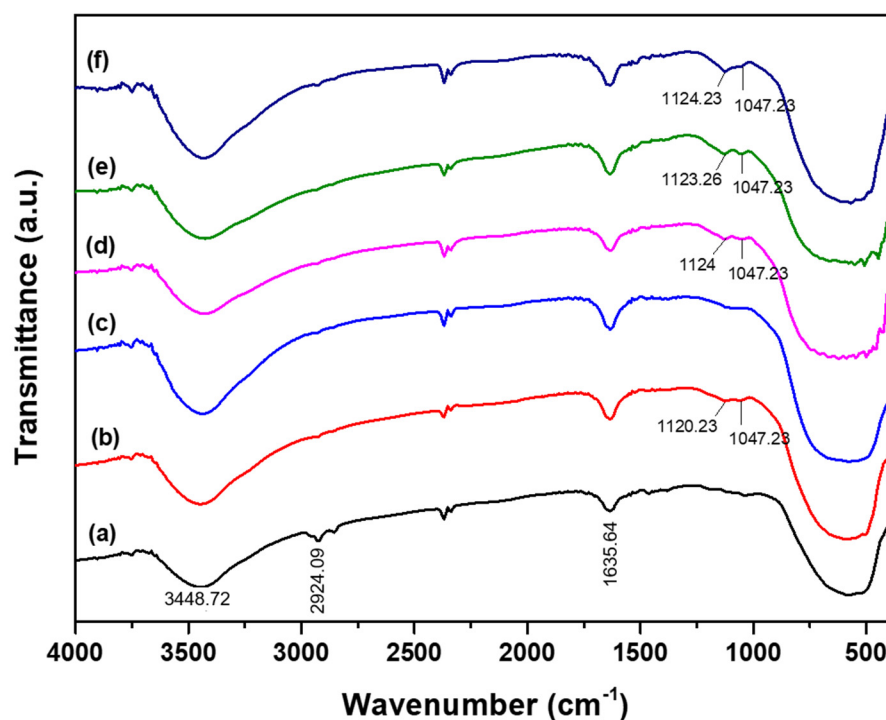


**Figure 2.** FTIR spectra of (a) pure  $\text{TiO}_2$ , (b)  $\text{S-TiO}_2$ , (c)  $\text{Co-TiO}_2$ , (d)  $\text{S-Co-TiO}_2$  4%, (e)  $\text{S-Co-TiO}_2$  6%, and (f)  $\text{S-Co-TiO}_2$  8%.

### 3.1.3. SEM Analysis

SEM analysis was used to identify the surface morphology of the photocatalysts, and the SEM micrographs of undoped, doped, and co-doped  $\text{TiO}_2$  are presented in Figure 3. The surface of pure  $\text{TiO}_2$  showed a uniform spherical morphology and size homogeneity. After being modified with Co dopant, the photocatalyst showed a surface with large and inhomogeneous agglomerates, while after co-doped with S and Co, the particles formed homogeneous spherical agglomerates with smaller sizes.

EDX was employed to classify the elemental composition of the photocatalyst. The EDX pattern confirmed the presence of S, Co, or both dopants in the  $\text{S-TiO}_2$ ,  $\text{Co-TiO}_2$ , or co-doped  $\text{TiO}_2$  samples in addition to the main elements Ti and O (Figure 3). A small amount of sulfur could not be identified in the  $\text{S-Co-TiO}_2$  4% sample, which may be due to the dopants' content being too small. Other than that, the EDX pattern confirmed that all the targeted elements are in the  $\text{TiO}_2$  co-doped sample (Table 2).

**Table 2.** The elemental composition of undoped  $\text{TiO}_2$ ,  $\text{S-TiO}_2$ ,  $\text{Co-TiO}_2$ , and  $\text{S-Co-TiO}_2$ .

Element	% Atom					
	$\text{TiO}_2$	$\text{S-TiO}_2$	$\text{Co-TiO}_2$	$\text{S-Co-TiO}_2$ 4%	$\text{S-Co-TiO}_2$ 6%	$\text{S-Co-TiO}_2$ 8%
Ti	27.28	22.53	29.07	21.26	20.93	22.94
O	72.72	77.37	69.35	78.37	78.60	76.25
S	-	0.10	-	-	0.09	0.17
Co	-	-	1.58	0.38	0.39	0.63

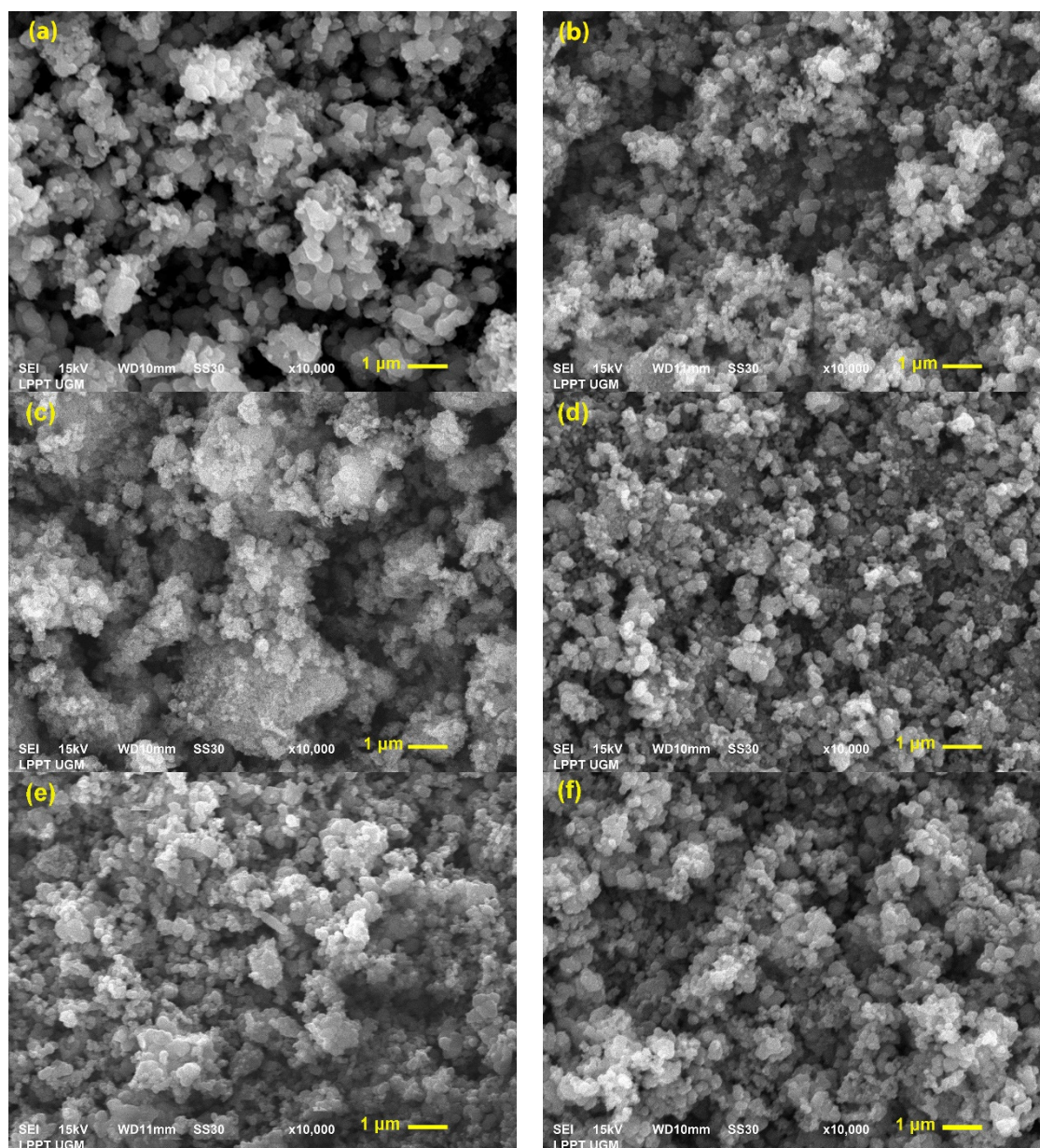


**Figure 3.** SEM images of (a) pure TiO<sub>2</sub>, (b) S-TiO<sub>2</sub>, (c) Co-TiO<sub>2</sub>, (d) S-Co-TiO<sub>2</sub> 4%, (e) S-Co-TiO<sub>2</sub> 6%, and (f) S-Co-TiO<sub>2</sub> 8%.

#### 3.1.4. UV-Vis SRS Analysis

The UV-Vis SRS spectrum revealed the optical properties and band gap energy of the photocatalyst. Figure 4 exhibits the UV-Vis SRS spectrum and Tauc's plot of undoped, doped, and co-doped TiO<sub>2</sub>. As shown in Figure 4a, TiO<sub>2</sub> shows an ultraviolet absorption semiconductor profile (200–400 nm) due to the large band gap energy of anatase TiO<sub>2</sub> (3.2 eV). A small red-shift to the visible region was observed in the S-TiO<sub>2</sub> sample due to the formation of a new sub-band gap in the valence band (VB) from the formation of the Ti–O–S bond after S doped to titania [37]. The new sub-band gap is formed by mixing the S<sub>3p</sub> orbital with the O<sub>2p</sub> orbital, which narrows the band gap of TiO<sub>2</sub> [25]. The distinctive red-shift was also observed in the Co-TiO<sub>2</sub> sample, indicating that Co-TiO<sub>2</sub> has an absorption in the visible region. The optical absorption mechanism of undoped TiO<sub>2</sub> is the transition energy from the valence band to the conduction band. The sp-d exchange interaction between the band electrons and the localized d-electrons of the Co<sup>2+</sup> ion replacing the Ti<sup>4+</sup> cation is responsible for the red-shift in the Co-TiO<sub>2</sub> sample. This

interaction between sp and pd causes a downward shift in the conduction band (CB) and an upward shift in VB, narrowing the band gap system [38].

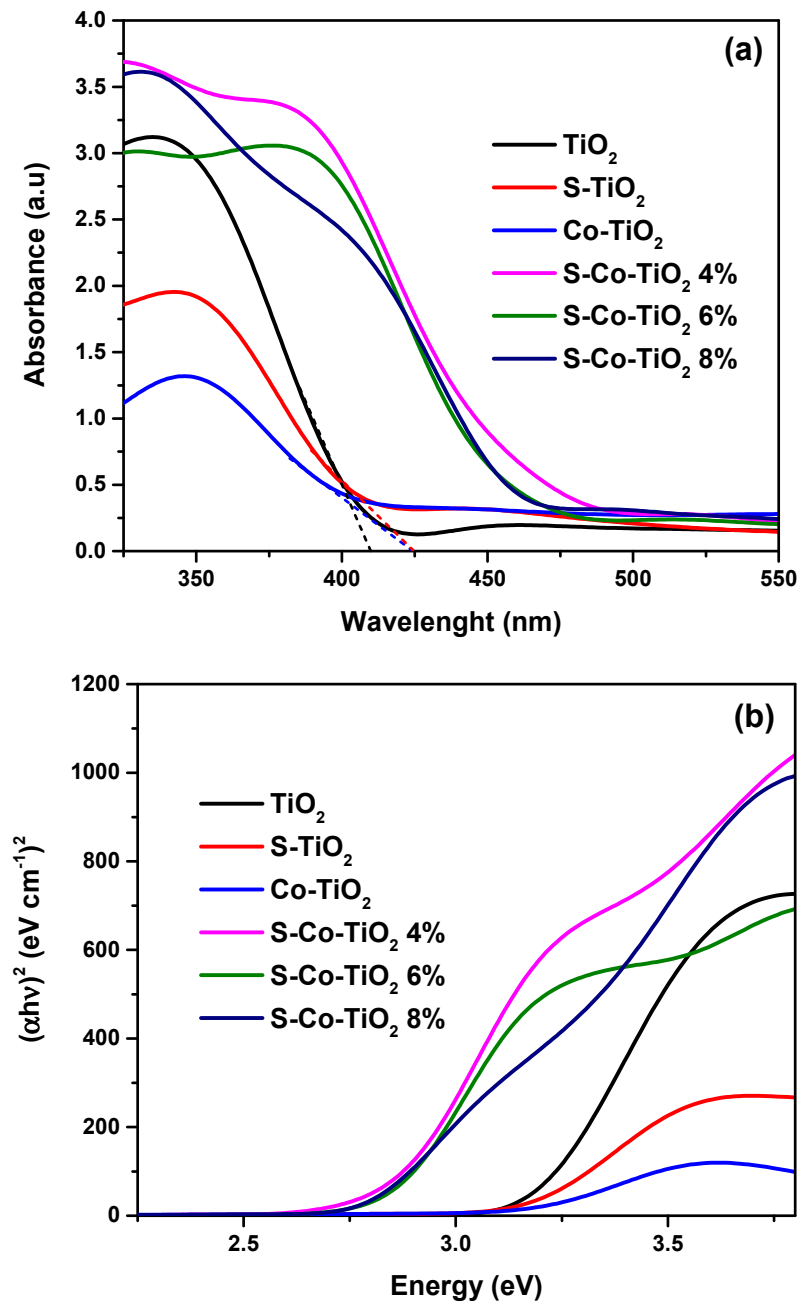


Figure 4. (a) UV-Vis SRS spectrum and (b) Tauc's plot of prepared photocatalysts.

Meanwhile, the red shift in the co-doping sample ( $\text{S-Co-TiO}_2$ ) was the most significant compared to the previous two doping samples ( $\text{S-TiO}_2$  or  $\text{Co-TiO}_2$ ). The  $\text{S-Co-TiO}_2$  sample displayed a high adsorption profile in the ultraviolet region, even higher than undoped and doped  $\text{TiO}_2$ . Then, the absorption bands are significantly widened to the visible light region, implying that the photocatalyst activity in visible light has increased due to the impurity of S and Co co-dopants in  $\text{TiO}_2$ . The SRUV-Vis absorption data were implemented into a Tauc's plot between  $(\alpha h\nu)^2$  versus  $h\nu$  to determine the band gap energy before and after modification, and the results are presented in Figure 4b. The band gap energy of undoped  $\text{TiO}_2$  was identified to be 3.2 eV. When impurity S is present in  $\text{TiO}_2$ , the band gap is reduced to 3.16 eV, while doping by Co lowered the band gap to 3.15 eV. The

decrease in band gap energy was more significant when  $\text{TiO}_2$  was co-doped by S and Co. The addition of 4% and 6%  $\text{CoSO}_4$  as a single precursor of co-dopants caused a decrease in the band gap to 2.82 and 2.83, respectively. The most significant decrease occurred at the S-Co- $\text{TiO}_2$  8% sample, resulting in a band-gap width of 2.78 eV (Table 1). The more significant band-gap narrowing in the co-doped sample may be due to the formation of two impurity states close to the VB and CB. One is formed by mixing the  $\text{S}_{3p}$  orbitals with the  $\text{O}_{2p}$  orbitals of the S dopant, and the other is formed by exchange interactions between the sp on the electrons band and d-electrons of the  $\text{Co}^{2+}$  ion that replaces the  $\text{Ti}^{4+}$  ion [25,38,39].

### 3.2. Photocatalytic Performance on RBB Removal

#### 3.2.1. Effect of Different Photocatalyst

The prepared photocatalysts  $\text{TiO}_2$ , S- $\text{TiO}_2$ , Co- $\text{TiO}_2$ , and S-Co- $\text{TiO}_2$ , were used in the photocatalytic removal of RBB under visible or UV-light irradiation separately to evaluate the photocatalytic activity before and after modification. In this experiment,  $20 \text{ mg L}^{-1}$  of RBB solution was added with the prepared photocatalyst and then irradiated with visible/UV light for a certain time. The results of RBB removal using various photocatalysts are shown in Figure 5.

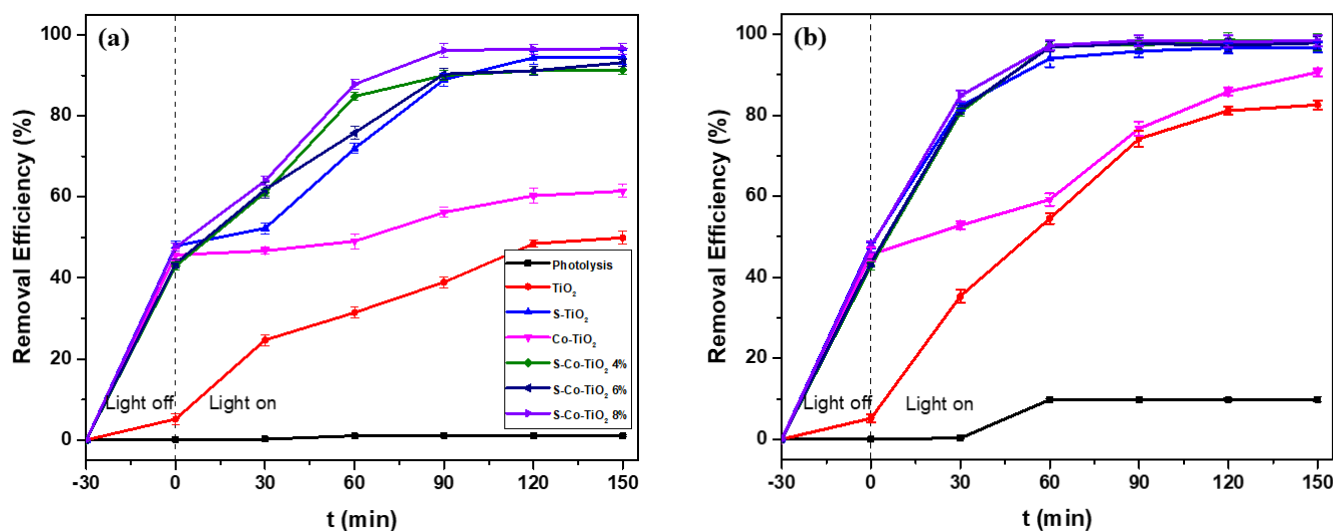


**Figure 5.** The effect of various photocatalysts on the removal efficiency of RBB using (a) visible, and (b) UV-light irradiation, RBB concentration:  $20 \text{ mg L}^{-1}$ , photocatalyst dosage:  $1 \text{ g L}^{-1}$ , and pH: 5.5.

In order to determine the photolysis properties of RBB, the removal concentration without the addition of the photocatalyst was also investigated. The results showed that RBB did not undergo photolysis after 150 min of UV or visible light exposure.

Figure 5a shows the photocatalytic activity of various prepared photocatalysts under visible light. A reasonably good result is shown in the S- $\text{TiO}_2$  sample. The undoped  $\text{TiO}_2$  was only able to degrade 49% of RBB after 150 min of visible light exposure. Meanwhile, after dopant addition, the removal efficiency of RBB increased to 94% and 61% for S- $\text{TiO}_2$  and Co- $\text{TiO}_2$  after 120 min of exposure, respectively. However, the most effective removal of RBB was obtained from the  $\text{TiO}_2$  co-doped by S and Co 8% (S-Co- $\text{TiO}_2$  8%) photocatalyst. Although S- $\text{TiO}_2$  reduced 94% of dye concentration, time efficiency can be achieved in co-doped samples (S-Co- $\text{TiO}_2$  8%), which can remove 96% of RBB in 90 min of visible light irradiation. Thus, the S-Co- $\text{TiO}_2$  8% demonstrated the best photocatalytic performance compared to other prepared photocatalysts.

Under UV irradiation, the S-Co- $\text{TiO}_2$  8% sample also demonstrated the highest photocatalytic activity compared to other photocatalysts. During 90 min of UV irradiation, 98% of RBB could be removed, while S- $\text{TiO}_2$ , Co- $\text{TiO}_2$ , and pure  $\text{TiO}_2$  removed 95%, 76%, and 74% of RBB concentration, respectively. These findings confirm that S-and-Co-co-doped

TiO<sub>2</sub> (S-Co-TiO<sub>2</sub>) exhibits the most significant increase in photocatalytic activity in visible or UV light.

Pure TiO<sub>2</sub> displayed significant photocatalytic activity in UV light but not in visible light since the energy from visible light is insufficient to activate TiO<sub>2</sub>. The UV light energy corresponds to the expansive band-gap energy of TiO<sub>2</sub> (3.2 eV). However, the presence of S and Co as impurity dopants in the titania structure can enhance the photocatalytic activity in visible light due to the formation of new sub-levels energy in the titania structure, resulting in a narrowing of the TiO<sub>2</sub> band gap energy [25]. The new energy level formed by the S atom was attributed to the substitution of Ti<sup>4+</sup> by S<sup>6+</sup> from mixing the S<sub>3p</sub> orbital with the O<sub>2p</sub> orbital close to the valence band (VB), which narrowed the band gap of TiO<sub>2</sub> and increased the absorption of visible light [13,25,29]. On the other hand, Co dopant contributes to lowering the band gap energy from the substitution of Ti<sup>4+</sup> by Co<sup>2+</sup>. Co dopant directs the sp-d exchange interaction between the band electrons and localized d-electrons of the Co<sup>2+</sup> ion that replace the Ti<sup>4+</sup> ion. This interaction causes a downward shift of the conduction band (CB), resulting in a narrowing of the band gap system [25,30,38]. The synergetic effect of S and Co dopants forming two new energy levels on the S-Co-TiO<sub>2</sub> sample resulted in the most optima in decreasing the band gap energy and encouraging the visible-light absorption compared to S-TiO<sub>2</sub> or Co-TiO<sub>2</sub> samples.

Although both were doped, S-TiO<sub>2</sub> had a much higher photocatalytic activity than Co-TiO<sub>2</sub>. According to the literature, the higher activity of S-TiO<sub>2</sub> can be attributed to the presence of hydroxyl groups on the surface of the sulfur oxide photocatalyst, which can create an acidic environment on the surface. Then, the substitution of Ti<sup>4+</sup> by S<sup>6+</sup> ions in the TiO<sub>2</sub> lattice causes a charge imbalance in the structure of TiO<sub>2</sub>. The extra positive charge formed will attract anions from the solution, such as hydroxide ions, to the surface of the photocatalyst, thereby neutralizing the charge imbalance [40]. Furthermore, this extra positive charge can adsorb the h<sub>vb</sub><sup>+</sup> formed by the photocatalyst induced by light to produce hydroxyl radicals, which have strong oxidizing power to decompose the organic compounds such as RBB dyes. The difference in electronegativity between the S and O atoms in the Ti-O-S bond causes electron transfer from the less electronegative S atom to the more electronegative O atom. This causes the sulfur atom to be deprived of electrons and will retain e<sup>-</sup> generated by the photocatalyst. As a result, the electron and hole recombination rate decreases, and h<sub>vb</sub><sup>+</sup> will be abundantly available to generate more hydroxyl radicals on the surface of the photocatalyst [13]. The abundant availability of hydroxyl radicals will increase the decontamination efficiency of organic compounds such as RBB dyes.

The co-doped samples demonstrated the most superior photocatalytic activity in visible or UV-light due to a variety of factors, including a better narrowing in band gap, a decrease in particle size, and an increase in surface-area-reduced electron and hole recombination [15,41]. This result is in accordance with the band gap energy (E<sub>g</sub>) obtained from the UV-vis SRS data, such that S-Co-TiO<sub>2</sub> 8% produces the most significant decrease in E<sub>g</sub>, which is 2.78 eV and corresponds to the energy of visible light irradiation.

The decolorization process by the photocatalyst starts with the surface adsorption process and continues with the photocatalytic reaction. In order to evaluate the surface adsorption properties of the S-Co-TiO<sub>2</sub> 8% photocatalyst as well as to evaluate whether the adsorption process continued along with the photocatalytic process, the adsorption of the S-Co-TiO<sub>2</sub> 8% catalyst was carried out in the dark for 150 min without irradiation as shown in Figure 6. The undoped TiO<sub>2</sub> adsorption test was also used for comparison purposes. The results indicate that adsorption takes place in the first 15 min and the concentration of the dye tends not to decrease, which implies that the next process is photocatalytic decolorization after a contact period of 15 min.

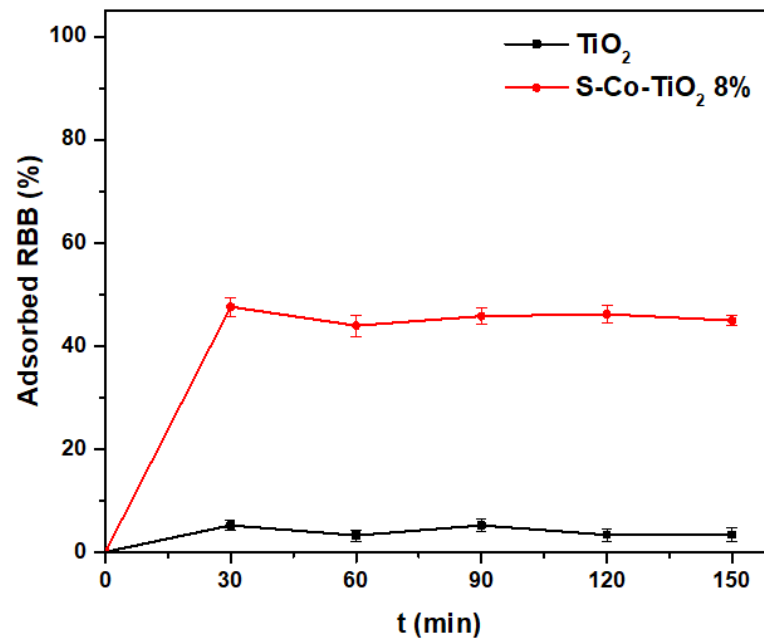


**Figure 6.** Adsorption of RBB by TiO<sub>2</sub> and S-Co-TiO<sub>2</sub> 8% in the dark condition at RBB concentration: 20 mg L<sup>-1</sup>, photocatalyst dosage: 1 g L<sup>-1</sup>, and initial pH: 5.5.

### 3.2.2. Effect of pH

The effect of pH is a critical parameter in the efficiency of the decolorization process because it can affect the photocatalyst surface, dye characteristics, and the rate of decolorization. As shown in Figure 7, the effect of the initial pH on RBB removal by the S-CoTiO<sub>2</sub> 8% catalyst under 60 min of visible light exposure was evaluated in the range of 2.0–10.0.

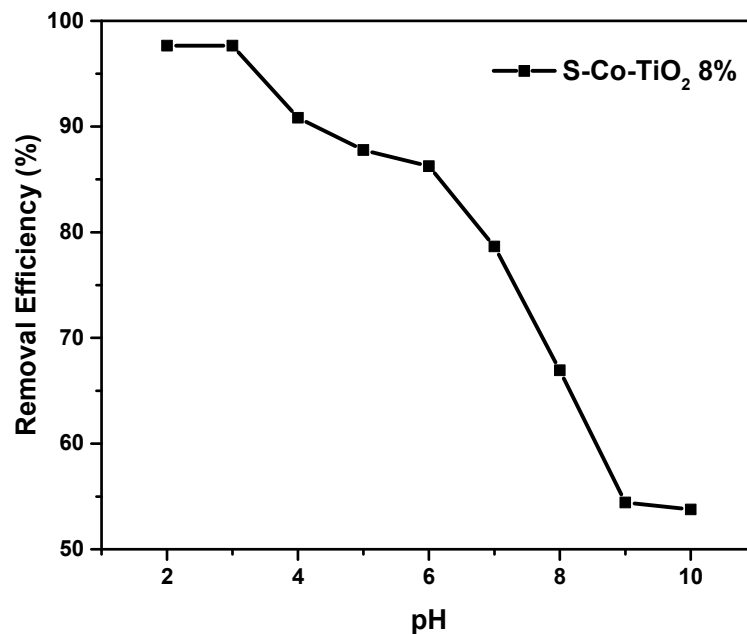


**Figure 7.** Influence of pH on photocatalytic decolorization of RBB under 60 min of visible light irradiation by the S-Co-TiO<sub>2</sub> 8% photocatalyst, RBB concentration: 20 mg L<sup>-1</sup>, photocatalyst dosage: 1 g L<sup>-1</sup>.

As shown in Figure 7, when the initial pH was reduced from 5.0 to 3.0, the decolorization efficiency of RBB increased from 88% to 97% at 60 min of irradiation. However, there was no increase in decolorization when the pH was reduced to 2.0. However, increasing

the solution pH to 8.0, 9.0, and 10.0 reduced the decolorization efficiency to 67%, 54%, and 53%, respectively. This result can be explained by the fact that  $\text{TiO}_2$  has a positive or negative charge depending on the pH of the solution:



The optimum pH for RBB decolorization was found to be 3.0, and the  $\text{pH}_{\text{PZC}}$  of S-Co-TiO<sub>2</sub> 8% was found to be 6.41 (Figure 8). When the solution pH is below the  $\text{pH}_{\text{PZC}}$ , the  $\text{TiO}_2$  surface will be positively charged. At acidic medium (pH = 3.0), RBB has sulfonate ( $\text{SO}_3^-$ ) and sulfite ( $\text{SO}_3^{2-}$ ) groups, which can be adequately adsorbed by the positive charge on the surface of  $\text{TiO}_2$  through electrostatic force at the beginning of the decolorization process [3,42]. As a result, the optimal pH of RBB adsorption on the catalyst surface is 3.0. When the pH of the solution is lowered from 7.0 to 10.0, the removal efficiency decreases as well. It can be explained because at alkaline pH conditions, the surface of  $\text{TiO}_2$  is negatively charged, leading to charge repulsion with the RBB, which is also negative.

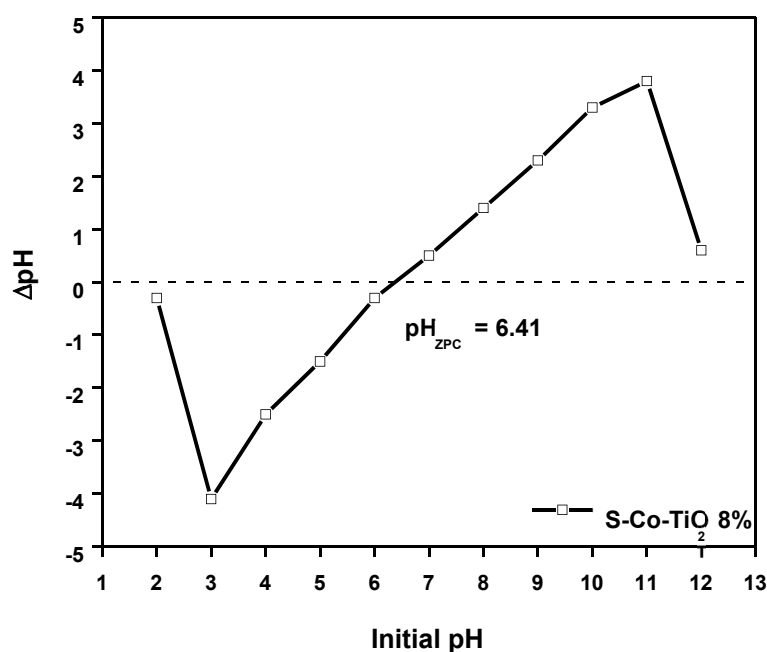
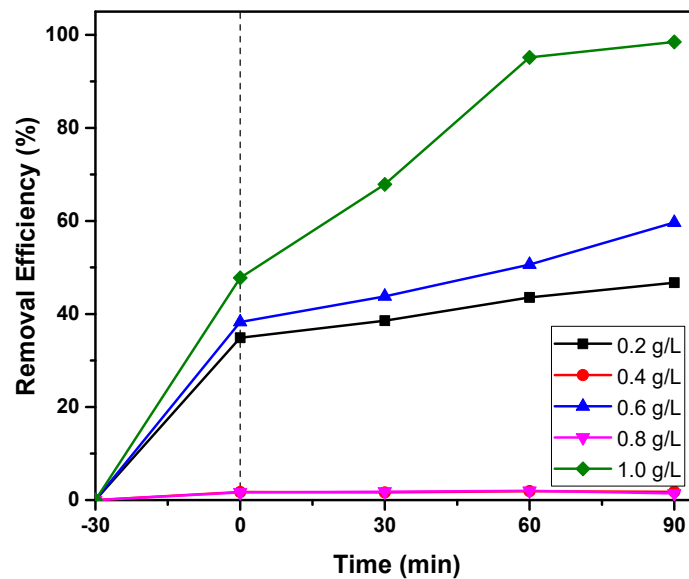


Figure 8.  $\text{pH}_{\text{PZC}}$  of the S-Co-TiO<sub>2</sub> 8% photocatalyst.

### 3.2.3. Effect of Catalyst Dosage

The effect of photocatalyst amount on the RBB removal under visible light irradiation was investigated by varying the mass of the S-Co-TiO<sub>2</sub> 8% from 0.2 to 1.0 g L<sup>-1</sup> ( $C_0 = 20 \text{ mg L}^{-1}$ , pH = 3.0). The obtained results are shown in Figure 9.

As shown in Figure 9, increasing the photocatalyst mass from 0.2 to 1.0 mg L<sup>-1</sup> resulted in additional RBB removal, which was associated with an increased adsorption rate on the catalyst surface and increased hydroxyl radical formation. The photocatalyst mass of 1.0 g L<sup>-1</sup> provided the highest decolorization efficiency. However, the amount of dye adsorbed on the surface of the photocatalyst was very high at the beginning of the reaction, whereas the photocatalytic reaction became insignificant. It can be seen that after 60 min of irradiation, the photocatalytic reaction did not continue since an excessive amount of photocatalyst had increased the number of active sites on the surface of the photocatalyst, allowing adsorption to dominate at the start of the process while the photocatalytic reaction becomes insignificant.



**Figure 9.** The effect of the S-Co-TiO<sub>2</sub> 8% photocatalyst dosage on RBB removal at RBB concentration: 20 mg L<sup>-1</sup> and initial pH: 3.0.

The photocatalyst mass of 0.6 mg L<sup>-1</sup> was chosen for further investigation due to its high photocatalytic efficiency after 30 min of adsorption–desorption. When the photocatalyst dosage was increased from 0.6 to 1.0 mg L<sup>-1</sup>, decolorization was almost insignificantly different.

### 3.2.4. Effect of Dye Concentration

The color removal process is affected by the initial concentration of pollutants. Therefore, the effect of RBB concentration on the efficiency of decolorization by the S-Co-TiO<sub>2</sub> 8% photocatalyst was carried out by varying the RBB concentration from 20 to 50 mg L<sup>-1</sup>, and the results obtained are presented in Figure 10. The decolorization efficiency decreased from 98% to 57% as the RBB concentration increased from 20 mg L<sup>-1</sup> to 50 mg L<sup>-1</sup>. This is due to the fact that as the dye concentration increases, the number of molecules adsorbed on the photocatalyst surface increases, obstructing direct contact with the holes and inhibiting the formation of hydroxyl radicals. Furthermore, at higher concentrations, the dye molecules adsorbed more photons, thereby reducing the light intensity and decolorization efficiency [28,43].

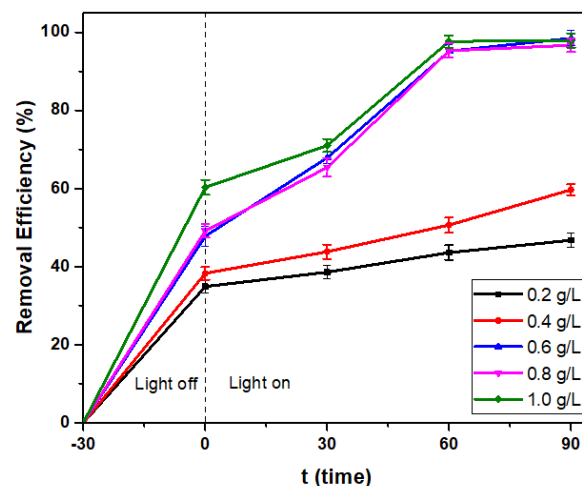


**Figure 10.** The effect of RBB concentration on S-Co-TiO<sub>2</sub> 8% dose 0.6 g L<sup>-1</sup>, initial pH: 3.0, and 90 min of visible light irradiation.

### 3.2.5. The Recyclable Ability of S-Co-TiO<sub>2</sub> 8% Photocatalyst

The stability and reusability of photocatalysts are critical parameters in the study of photocatalysts for use in sustainable wastewater treatment. The S-Co-TiO<sub>2</sub> 8% photocatalyst was tested for stability and reuse four times. In each test, S-Co-TiO<sub>2</sub> 8% was centrifuged and then washed and dried before being used in the next cycle under the same experimental conditions for 90 min of visible light irradiation. The reuse test results for S-Co-TiO<sub>2</sub> 8% photocatalyst are shown in Figure 11. The results showed that the S-Co-TiO<sub>2</sub> 8% sample had high decolorization efficiency after four reuse cycles, but there was a 44% decrease in decolorization efficiency after four uses. This could be due to the loss of photocatalyst during the iteration process. These findings suggest that the co-doped sample S-Co-TiO<sub>2</sub> 8% photocatalyst has promising potential and can be used repeatedly to remove dye pollutants.

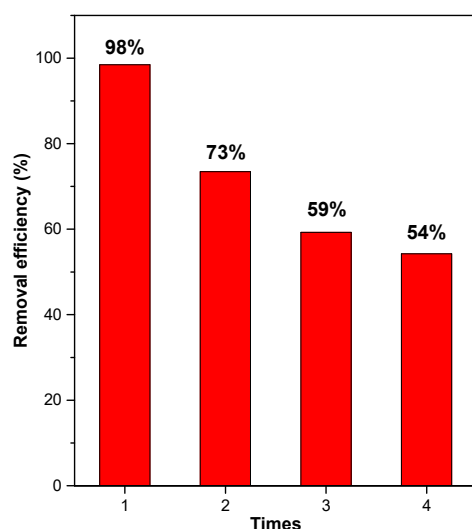
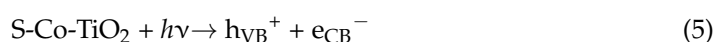


**Figure 11.** Recyclability of S-Co-TiO<sub>2</sub> 8% for RBB removal under visible light illumination, RBB concentration: 20 mg L<sup>-1</sup>, initial pH: 3.0, and photocatalyst dosage: 0.6 g L<sup>-1</sup>.

### 3.3. Mechanism of RBB Photocatalytic Decolorization

Photocatalytic removal reactions can occur when TiO<sub>2</sub> absorbs photons with energies equal to or greater than their band gap energy. S and Co co-dopants create impurity states close to VB and CB, resulting in a narrowing of the TiO<sub>2</sub> band gap, thereby increasing photocatalytic visible light activity. The schematic of the S-Co-TiO<sub>2</sub> photocatalyst mechanism is presented in Figure S6. The characterization results using XRD, FTIR, SEM-EDX, and SRS UV-vis indicate that the modification of the addition of S and Co co-dopants to TiO<sub>2</sub> has been successfully carried out.

When S-Co-TiO<sub>2</sub> is exposed to visible light radiation, electrons in the VB are excited towards the CB (e<sub>CB</sub><sup>-</sup>), producing holes (h<sub>VB</sub><sup>+</sup>) in the VB. These excited electron-hole pairs are commonly referred to as excitons [44]. The mechanism that occurs is as follows:



The holes can react with adsorbed hydroxyl anion on the TiO<sub>2</sub> surface to form hydroxyl radicals, which have high oxidizing power and can decompose organic pollutants, and excited electrons (e<sub>CB</sub><sup>-</sup>) can reduce O<sub>2</sub> to form oxygen radicals, which can be converted into hydroxyl radicals in water as follows:



#### 4. Conclusions

The decolorization of Remazol Black (RBB) was investigated using an S-Co-TiO<sub>2</sub> photocatalyst. This photocatalyst was prepared through one-pot synthesis using a single precursor as a source of S and Co dopants. Characterization using XRD, FT-IR, SEM-EDX, and UV-Vis SRS showed that S-and-Co co-doped TiO<sub>2</sub> was successfully synthesized and degraded RBB under visible light better than TiO<sub>2</sub> or S-TiO<sub>2</sub> and Co-TiO<sub>2</sub>. Eight percent (*w/w*) of CoSO<sub>4</sub> as a single precursor of S and Co provides the best reduction in band gap energy to 2.78 eV and is supported by the best photocatalytic activity when compared to other photocatalysts. After 90 min of temporary visible light, the S-Co-TiO<sub>2</sub> 8% can degrade 96% of RBB, whereas S-TiO<sub>2</sub>, Co-TiO<sub>2</sub>, and undoped TiO<sub>2</sub> can decrease to 89%, 56%, and 39%, respectively, and the optimum decolorization results are obtained at pH 3.0. Reuse studies show that S-Co-TiO<sub>2</sub> 8% has the potential to be used repeatedly for the removal of dye pollutants in the environment.

**Supplementary Materials:** The following are available online at <https://www.mdpi.com/article/10.3390/photochem1030032/s1>, Figure S1: Chemical structure of Remazol Black (RBB); Figure S2: Schematic diagram of photoreactor for photocatalytic experiment; Figure S3: EDX pattern of (a) TiO<sub>2</sub>, (b) S-TiO<sub>2</sub>, (c) Co-TiO<sub>2</sub>, (d) S-Co-TiO<sub>2</sub> 4%, (e) S-Co-TiO<sub>2</sub> 6%, and (f) S-Co-TiO<sub>2</sub> 8%; Figure S4: Absorption spectrum of Remazol Black analyzed by spectrophotometry, Remazol Black concentration: 20 mg L<sup>-1</sup>; Figure S5: Spectrum of Remazol Black after decolorization by S-Co-TiO<sub>2</sub> 8% photocatalyst for 150 min visible light irradiation, photocatalyst dose: 1.0 g L<sup>-1</sup>, initial pH: 5.5, Remazol Black concentration: 20 mg L<sup>-1</sup>, Figure S6: Schematic diagram of photocatalytic decolorization of RBB by S-Co-TiO<sub>2</sub> photocatalyst.

**Author Contributions:** Conceptualization, E.T.W.; methodology, E.T.W. and R.D.; software, R.D.; validation, E.T.W., R.R. and R.D.; formal analysis, R.D., E.T.W. and R.R.; investigation, R.D., E.T.W. and R.R.; resources, R.D. and E.T.W.; data curation, R.D. and E.T.W.; writing—original draft preparation, R.D.; writing—review and editing, E.T.W., R.R. and R.D.; visualization, R.D., E.T.W. and R.R.; supervision, R.D.; project administration, E.T.W. and R.D.; funding acquisition, E.T.W. and R.D. All authors have read and agreed to the published version of the manuscript.

**Funding:** This research was financially supported by Kemenristekdikti (Ministry of Research, Technology and Higher Education) of Indonesia through the Pendidikan Magister menuju Doktor untuk Sarjana Unggul (PMDSU) Scholarship Program (contract No. 2335/UN1/DITLIT/DIT-LIT/PT/2021).

**Institutional Review Board Statement:** Not applicable.

**Informed Consent Statement:** Not applicable.

**Data Availability Statement:** All the data presented in this study are available in the article.

**Acknowledgments:** The first author is grateful to the Ministry of Research, Technology, and Higher Education of Indonesia (Kemenristekdikti) for providing a comprehensive scholarship to enable this research to be carried out, as well as to the Department of Chemistry, Universitas Gadjah Mada, which has provided this research facilities.

**Conflicts of Interest:** The authors declare no conflict of interest, and the funders had no role in the design of the study; in the collection, analyses, or interpretation of data; in the writing of the manuscript, or in the decision to publish the results.

#### References

1. Marques, S.M.; Tavares, C.J.; Oliveira, L.F.; Oliveira-Campos, A.M.F. Photocatalytic degradation of C.I. Reactive Blue 19 with nitrogen-doped TiO<sub>2</sub> catalysts thin films under UV/visible light. *J. Mol. Struct.* **2010**, *983*, 147–152. [CrossRef]
2. Ahmad, M.A.; Rahman, N.K. Equilibrium, kinetics and thermodynamic of Remazol Brilliant Orange 3R dye adsorption on coffee husk-based activated carbon. *Chem. Eng. J.* **2011**, *170*, 154–161. [CrossRef]
3. Muruganandham, M.; Sobana, N.; Swaminathan, M. Solar assisted photocatalytic and photochemical degradation of Reactive Black 5. *J. Hazard. Mater.* **2006**, *137*, 1371–1376. [CrossRef]
4. Sahel, K.; Perol, N.; Dappozze, F.; Bouhent, M.; Derriche, Z.; Guillard, C. Photocatalytic degradation of a mixture of two anionic dyes: Procion Red MX-5B and Remazol Black 5 (RB5). *J. Photochem. Photobiol. A Chem.* **2010**, *212*, 107–112. [CrossRef]

5. Chen, C.Y.; Cheng, M.C.; Chen, A.H. Photocatalytic decolorization of Remazol Black 5 and Remazol Brilliant Orange 3R by mesoporous TiO<sub>2</sub>. *J. Environ. Manag.* **2012**, *102*, 125–133. [[CrossRef](#)]
6. de Oliveira Pereira, L.; Marques Sales, I.; Pereira Zampiere, L.; Silveira Vieira, S.; do Rosário Guimarães, I.; Magalhães, F. Preparation of magnetic photocatalysts from TiO<sub>2</sub>, activated carbon and iron nitrate for environmental remediation. *J. Photochem. Photobiol. A Chem.* **2019**, *382*, 111907. [[CrossRef](#)]
7. Behnajady, M.A.; Modirshahla, N.; Shokri, M.; Rad, B. Enhancement of photocatalytic activity of TiO<sub>2</sub> nanoparticles by Silver doping: Photodeposition versus liquid impregnation methods. *Glob. Nest J.* **2008**, *10*, 1–7. [[CrossRef](#)]
8. Wu, M.C.; Wu, P.Y.; Lin, T.H.; Lin, T.F. Photocatalytic performance of Cu-doped TiO<sub>2</sub> nanofibers treated by the hydrothermal synthesis and air-thermal treatment. *Appl. Surf. Sci.* **2018**, *430*, 390–398. [[CrossRef](#)]
9. Murcia, J.J.; Hidalgo, M.C.; Navío, J.A.; Araña, J.; Doña-Rodríguez, J.M. Study of the phenol photocatalytic degradation over TiO<sub>2</sub> modified by sulfation, fluorination, and platinum nanoparticles photodeposition. *Appl. Catal. B Environ.* **2015**, *179*, 305–312. [[CrossRef](#)]
10. Lin, Y.H.; Hsueh, H.T.; Chang, C.W.; Chu, H. The visible light-driven photodegradation of dimethyl sulfide on S-doped TiO<sub>2</sub>: Characterization, kinetics, and reaction pathways. *Appl. Catal. B Environ.* **2016**, *199*, 1–10. [[CrossRef](#)]
11. Ramacharyulu, P.V.R.K.; Praveen Kumar, J.; Prasad, G.K.; Sreedhar, B. Sulphur doped nano TiO<sub>2</sub>: Synthesis, characterization and photocatalytic degradation of a toxic chemical in presence of sunlight. *Mater. Chem. Phys.* **2014**, *148*, 692–698. [[CrossRef](#)]
12. McManamon, C.; O'Connell, J.; Delaney, P.; Rasappa, S.; Holmes, J.D.; Morris, M.A. A facile route to synthesis of S-doped TiO<sub>2</sub> nanoparticles for photocatalytic activity. *J. Mol. Catal. A Chem.* **2015**, *406*, 51–57. [[CrossRef](#)]
13. Bakar, S.A.; Ribeiro, C. A comparative run for visible-light-driven photocatalytic activity of anionic and cationic S-doped TiO<sub>2</sub> photocatalysts: A case study of possible sulfur doping through chemical protocol. *J. Mol. Catal. A Chem.* **2016**, *421*, 1–15. [[CrossRef](#)]
14. Chen, C.; Ma, W.; Zhao, J. Photocatalytic Degradation of Organic Pollutants by Co-Doped TiO<sub>2</sub> Under Visible Light Irradiation. *Curr. Org. Chem.* **2010**, *14*, 630–644. [[CrossRef](#)]
15. Nasir, M.; Xi, Z.; Xing, M.; Zhang, J.; Chen, F.; Tian, B.; Bagwasi, S. Study of synergistic effect of Ce- and S-codoping on the enhancement of visible-light photocatalytic activity of TiO<sub>2</sub>. *J. Phys. Chem. C* **2013**, *117*, 9520–9528. [[CrossRef](#)]
16. Sun, H.; Zhou, G.; Liu, S.; Ang, H.M.; Tadó, M.O.; Wang, S. Visible light responsive titania photocatalysts codoped by nitrogen and metal (Fe, Ni, Ag, or Pt) for remediation of aqueous pollutants. *Chem. Eng. J.* **2013**, *231*, 18–25. [[CrossRef](#)]
17. Wang, F.; Ma, Z.; Ban, P.; Xu, X. C, N and S codoped rutile TiO<sub>2</sub> nanorods for enhanced visible-light photocatalytic activity. *Mater. Lett.* **2017**, *195*, 143–146. [[CrossRef](#)]
18. Singaram, B.; Varadharajan, K.; Jeyaram, J.; Rajendran, R.; Jayavel, V. Preparation of cerium and sulfur codoped TiO<sub>2</sub> nanoparticles based photocatalytic activity with enhanced visible light. *J. Photochem. Photobiol. A Chem.* **2017**, *349*, 91–99. [[CrossRef](#)]
19. Sinhmar, A.; Setia, H.; Kumar, V.; Sobti, A.; Toor, A.P. Enhanced photocatalytic activity of nickel and nitrogen codoped TiO<sub>2</sub> under sunlight. *Environ. Technol. Innov.* **2020**, *18*, 100658. [[CrossRef](#)]
20. Niu, Y.; Xing, M.; Tian, B.; Zhang, J. Improving the visible light photocatalytic activity of nano-sized titanium dioxide via the synergistic effects between sulfur doping and sulfation. *Appl. Catal. B Environ.* **2012**, *115–116*, 253–260. [[CrossRef](#)]
21. Yan, X.; Yuan, K.; Lu, N.; Xu, H.; Zhang, S.; Takeuchi, N.; Kobayashi, H.; Li, R. The interplay of sulfur doping and surface hydroxyl in band gap engineering: Mesoporous sulfur-doped TiO<sub>2</sub> coupled with magnetite as a recyclable, efficient, visible light active photocatalyst for water purification. *Appl. Catal. B Environ.* **2017**, *218*, 20–31. [[CrossRef](#)]
22. Kumar, M.K.; Godavarthi, S.; Karthik, T.V.K.; Mahendhiran, M.; Hernandez-Eligio, A.; Hernandez-Como, N.; Agarwal, V.; Martinez Gomez, L. Green synthesis of S-doped rod shaped anatase TiO<sub>2</sub> microstructures. *Mater. Lett.* **2016**, *183*, 211–214. [[CrossRef](#)]
23. Zhang, D.; Chen, J.; Xiang, Q.; Li, Y.; Liu, M.; Liao, Y. Transition-Metal-Ion (Fe, Co, Cr, Mn, Etc.) Doping of TiO<sub>2</sub> Nanotubes: A General Approach. *Inorg. Chem.* **2019**, *58*, 12511–12515. [[CrossRef](#)] [[PubMed](#)]
24. Nguyen, T.M.H.; Bark, C.W. Synthesis of Cobalt-Doped TiO<sub>2</sub> Based on Metal-Organic Frameworks as an Effective Electron Transport Material in Perovskite Solar Cells. *ACS Omega* **2020**, *5*, 2280–2286. [[CrossRef](#)] [[PubMed](#)]
25. Siddiq, A.; Masih, D.; Anjum, D.; Siddiq, M. Cobalt and sulfur co-doped nano-size TiO<sub>2</sub> for photodegradation of various dyes and phenol. *J. Environ. Sci.* **2015**, *37*, 100–109. [[CrossRef](#)]
26. El Mragui, A.; Logvina, Y.; da Silva, L.P.; Zegaoui, O.; da Silva, J.C.G.E. Synthesis of Fe- and Co-doped TiO<sub>2</sub> with improved photocatalytic activity under visible irradiation toward carbamazepine degradation. *Materials* **2019**, *12*, 3874. [[CrossRef](#)]
27. Eskandari, P.; Farhadian, M.; Solaimany Nazar, A.R.; Jeon, B.H. Adsorption and Photodegradation Efficiency of TiO<sub>2</sub>/Fe<sub>2</sub>O<sub>3</sub>/PAC and TiO<sub>2</sub>/Fe<sub>2</sub>O<sub>3</sub>/Zeolite Nanophotocatalysts for the Removal of Cyanide. *Ind. Eng. Chem. Res.* **2019**, *58*, 2099–2112. [[CrossRef](#)]
28. Isari, A.A.; Payan, A.; Fattahi, M.; Jorfi, S.; Kakavandi, B. Photocatalytic degradation of rhodamine B and real textile wastewater using Fe-doped TiO<sub>2</sub> anchored on reduced graphene oxide (Fe-TiO<sub>2</sub> /rGO): Characterization and feasibility, mechanism and pathway studies. *Appl. Surf. Sci.* **2018**, *462*, 549–564. [[CrossRef](#)]
29. Yi, C.; Liao, Q.; Deng, W.; Huang, Y.; Mao, J.; Zhang, B.; Wu, G. The preparation of amorphous TiO<sub>2</sub> doped with cationic S and its application to the degradation of DCFs under visible light irradiation. *Sci. Total Environ.* **2019**, *684*, 527–536. [[CrossRef](#)]
30. Samet, L.; Ben Nasseur, J.; Chtourou, R.; March, K.; Stephan, O. Heat treatment effect on the physical properties of cobalt doped TiO<sub>2</sub> sol-gel materials. *Mater. Charact.* **2013**, *85*, 1–12. [[CrossRef](#)]

31. Chen, X.; Sun, H.; Zhang, J.; Guo, Y.; Kuo, D.H. Cationic S-doped TiO<sub>2</sub>/SiO<sub>2</sub> visible-light photocatalyst synthesized by co-hydrolysis method and its application for organic degradation. *J. Mol. Liq.* **2019**, *273*, 50–57. [[CrossRef](#)]
32. Das, K.; Sharma, S.N.; Kumar, M.; De, S.K. Morphology dependent luminescence properties of Co doped TiO<sub>2</sub> nanostructures. *J. Phys. Chem. C* **2009**, *113*, 14783–14792. [[CrossRef](#)]
33. Han, C.; Andersen, J.; Likodimos, V.; Falaras, P.; Linkugel, J.; Dionysiou, D.D. The effect of solvent in the sol-gel synthesis of visible light-activated, sulfur-doped TiO<sub>2</sub> nanostructured porous films for water treatment. *Catal. Today* **2014**, *224*, 132–139. [[CrossRef](#)]
34. Devi, L.G.; Kavitha, R. Enhanced photocatalytic activity of sulfur doped TiO<sub>2</sub> for the decomposition of phenol: A new insight into the bulk and surface modification. *Mater. Chem. Phys.* **2014**, *143*, 1300–1308. [[CrossRef](#)]
35. Mugundan, S.; Rajamannan, B.; Viruthagiri, G.; Shanmugam, N.; Gobi, R.; Praveen, P. Synthesis and characterization of undoped and cobalt-doped TiO<sub>2</sub> nanoparticles via sol-gel technique. *Appl. Nanosci.* **2015**, *5*, 449–456. [[CrossRef](#)]
36. Chen, Z.; Ma, J.; Yang, K.; Feng, S.; Tan, W.; Tao, Y.; Mao, H.; Kong, Y. Preparation of S-doped TiO<sub>2</sub>-three dimensional graphene aerogels as a highly efficient photocatalyst. *Synth. Met.* **2017**, *231*, 51–57. [[CrossRef](#)]
37. Abu Bakar, S.; Ribeiro, C. An insight toward the photocatalytic activity of S doped 1-D TiO<sub>2</sub> nanorods prepared via novel route: As promising platform for environmental leap. *J. Mol. Catal. A Chem.* **2016**, *412*, 78–92. [[CrossRef](#)]
38. Naseem, S.; Khan, W.; Khan, S.; Husain, S.; Ahmad, A. Consequences of (Cr/Co) co-doping on the microstructure, optical and magnetic properties of microwave assisted sol-gel derived TiO<sub>2</sub> nanoparticles. *J. Lumin.* **2019**, *205*, 406–416. [[CrossRef](#)]
39. Olowoyo, J.O.; Kumar, M.; Jain, S.L.; Shen, S.; Zhou, Z.; Mao, S.S.; Vorontsov, A.V.; Kumar, U. Reinforced photocatalytic reduction of CO<sub>2</sub> to fuel by efficient S-TiO<sub>2</sub>: Significance of sulfur doping. *Int. J. Hydrogen Energy* **2018**, *43*, 17682–17695. [[CrossRef](#)]
40. Yu, J.C.; Ho, W.; Yu, J.; Yip, H.; Po, K.W.; Zhao, J. Efficient visible-light-induced photocatalytic disinfection on sulfur-doped nanocrystalline titania. *Environ. Sci. Technol.* **2005**, *39*, 1175–1179. [[CrossRef](#)]
41. Chen, X.Q.; Su, Y.L.; Zhang, X.W.; Lei, L.C. Fabrication of visible-light responsive S-F-codoped TiO<sub>2</sub> nanotubes. *Chin. Sci. Bull.* **2008**, *53*, 1983–1987. [[CrossRef](#)]
42. Ghoreishian, S.M.; Badii, K.; Norouzi, M.; Rashidi, A.; Montazer, M.; Sadeghi, M.; Vafaei, M. Decolorization and mineralization of an azo reactive dye using loaded nano-photocatalysts on spacer fabric: Kinetic study and operational factors. *J. Taiwan Inst. Chem. Eng.* **2014**, *45*, 2436–2446. [[CrossRef](#)]
43. Ali, M.H.H.; Al-Afify, A.D.; Goher, M.E. Preparation and characterization of graphene—TiO<sub>2</sub> nanocomposite for enhanced photodegradation of Rhodamine-B dye. *Egypt. J. Aquat. Res.* **2018**, *44*, 263–270. [[CrossRef](#)]
44. Islam, M.T.; Dominguez, A.; Turley, R.S.; Kim, H.; Sultana, K.A.; Shuvo, M.A.I.; Alvarado-Tenorio, B.; Montes, M.O.; Lin, Y.; Gardea-Torresdey, J.; et al. Development of photocatalytic paint based on TiO<sub>2</sub> and photopolymer resin for the degradation of organic pollutants in water. *Sci. Total Environ.* **2020**, *704*, 135406. [[CrossRef](#)] [[PubMed](#)]